Combining Experiments for the Identification of the Parameters of Viscoelastic Materials

M. Schmelzer
Physikalisch-Technische Bundesanstalt, Germany, Email: martin.schmelzer@ptb.de

Introduction

The influence of material damping on sound reduction can be examined using model scale test facilities [1]. To do this, dynamically proper model scale materials are needed. Candidates such as acrylic glass and silicone show linear viscoelastic effects.

For materials of that type, there are several standardised measurement methods to acquire the dynamic properties, e.g. [2, 3, 4, 5]. Usually, these methods feature easy applicability, but only yield results tied to the measurement situation and are, therefore, of limited usability. This lack is caused by the impurity of the strain (compression, shear, elongation, etc.) throughout the macroscopic sample. Therefore, [2] distinguishes between different moduluses according to the experimental set-ups used and [3] defines form functions for correction when using special sample geometries.

Other types of measurement methods have been developed to improve the significance of the results, e.g. [6, 7, 8, 9]. They use mathematical models to calculate the spatial distribution of different strain types inside the sample. Thereby, the infinitesimal material properties are embedded into the system and can be accessed for the identification, independent of shape and load of the system.

Mostly these improved methods use one experimental set-up to gain their results. This paper presents an extension of that method type: Different set-ups are combined to gain comprehensive information about the test material.

Viscoelasticity

Linear viscoelasticity can be described in numerous ways, using convolution integrals, inner variables, frequency-dependent moduluses and more, see e.g. [6, 7, 8, 10, 11]. When using convolution integrals, the correlation between the stress tensor σ_{jk} and the strain tensor ε_{lm} is given by the tensor of memory functions M_{jklm}. For the simplicity of the formulas, spatial variables $\vec{x}$ will be omitted:

$$\sigma_{jk}(t) = \int_{\tau=-\infty}^{t} M_{jklm}(t-\tau)\, \dot{\varepsilon}_{lm}(\tau)\, d\tau. \qquad (1)$$

If the material is isotropic, then M_{jklm} only depends on two functions, e.g. K for compression and G for shear.

When the strain tensor ε_{lm} is expressed by the displacement u_j:

$$\varepsilon_{lm} = \frac{1}{2}\left(\frac{\partial u_l}{\partial x_m} + \frac{\partial u_m}{\partial x_l}\right), \qquad (2)$$

and the independent memory functions K und G are given by the ansatz (Prony series):

$$K(t) = \sum_{p=0}^{n} K_p\, e^{-b_p\, t} \quad ; \quad G(t) = \sum_{p=0}^{n} G_p\, e^{-b_p\, t}, \qquad (3)$$

with positive constants K_p, G_p and b_p, and when the convolution integral is treated with integration by parts, then the stress tensor σ_{jk} becomes:

$$\begin{aligned} \sigma_{jk} &= \sum_{p=0}^{n}\left[(K_p - \frac{2}{3}G_p)\,\delta_{jk}\sum_{m=1}^{3}\frac{\partial(u_m - y_{m,p})}{\partial x_m}\right] \qquad (4)\\ &+ \sum_{p=0}^{n}\left[G_p\left(\frac{\partial(u_j - y_{j,p})}{\partial x_k} + \frac{\partial(u_k - y_{k,p})}{\partial x_j}\right)\right] \\ \dot{y}_{j,p} &= b_p(u_j - y_{j,p}) \quad , \quad p = 0, \ldots, n. \qquad (5) \end{aligned}$$

The entities $y_{j,p}$ are inner variables of a displacement type, which originate – simply by definition – from the remaining integrals. δ_{jk} is the Kronecker symbol. Usually, b_0 is defined as zero. Then, K_0 and G_0 are the static moduluses known from linear elasticity (Hooke's law). The equations (4) and (5) provide an easy way to transfer a known elastic problem to a viscoelastic problem.

In the case of harmonic signals of the $e^{i\,\Omega\,t}$ type with the angular frequency Ω and $i = \sqrt{-1}$, elimination of the inner variables yields a formula for the complex amplitudes of stress $\hat{\sigma}_{jk}(\Omega)$ and displacement $\hat{u}_j(\Omega)$:

$$\begin{aligned} \hat{\sigma}_{jk}(\Omega) &= \left[K(\Omega) - \frac{2}{3}G(\Omega)\right]\left(\delta_{jk}\sum_{m=1}^{3}\frac{\partial \hat{u}_m(\Omega)}{\partial x_m}\right) \qquad (6)\\ &+ G(\Omega)\left(\frac{\partial \hat{u}_j(\Omega)}{\partial x_k} + \frac{\partial \hat{u}_k(\Omega)}{\partial x_j}\right), \end{aligned}$$

with the complex moduluses

$$K(\Omega) = \sum_{p=0}^{n} K_p\,\frac{i\Omega}{i\Omega + b_p} \qquad (7)$$

$$G(\Omega) = \sum_{p=0}^{n} G_p\,\frac{i\Omega}{i\Omega + b_p}. \qquad (8)$$

The real and imaginary parts are named storage and loss modulus, respectively. The same set of parameters K_p, G_p and b_p simultaneously describes the material in the time domain (3) and in the frequency domain (7) and (8).

Young's modulus E can be calculated from the moduluses in (7) and (8), see e.g. [12]:

$$E(\Omega) = \frac{9\,K(\Omega)\,G(\Omega)}{3\,K(\Omega) + G(\Omega)}. \qquad (9)$$

This way, certain conditions of thermodynamics are fulfilled automatically.

Identification

The parameters K_p, G_p and b_p and their number n must be determined individually for each material. Therefore, systems and measurands are chosen.

These systems are then realised experimentally and mathematically. Concerning the experimental set-ups, the chosen systems must enable an optimal experimental realisation of the exact mathematical boundary conditions and excitations. To avoid unknown influences from joints, it is recommended to choose free boundaries. Concerning the mathematical models, the experimentally occuring strain states should be as simple as possible to enable easy modeling.

Then, measurements and simulations are performed and their results are compared. The duration of excitation should be chosen to be as short as possible to avoid spontaneous heating of the samples. Short-time sweeps and maximum-length series were used. If accessible, analytical solutions of the equations of motion should be preferred to numerical solutions, as the latter usually require considerably more time to process.

The similarity of the compared measurements and simulations is expressed by a single number value. A search algorithm such as [13] repeats selecting parameters for the material, restarting the simulation, appraising the value of comparison and thereby routing the parameters to an optimum.

This paper now presents combined experiments for identification, i.e. ***multiple*** systems are chosen, but all of their simulations are based on ***one*** set of parameters. This one set of parameters will be valid for the material itself, regardless of the shape or load of the sample.

Experiments

One model scale material to be examined was silicone. To identify its parameters, two systems were chosen.

Rod specimen

The first system was a homogenous, finite rod with circular cross section, excited at one end and with a terminating mass at the other end. Figure 1 shows the set-up with the white silicone rod suspended from a shaker. The rod was excited using maximum-length series, which can be transformed to harmonic excitation. A uniaxial stress-strain state was supposed to develop inside the rod. So the well-known governing equation is

$$-\rho\,\Omega^2 u(\Omega, x) = E(\Omega) u''(\Omega, x), \qquad (10)$$

with Ω being the angular frequency and ρ the mass density. For the measurand, the transfer function of acceleration between the top and bottom surface of the rod was chosen. This was measured by the two accelerometers attached to the rod, and it can be easily calculated by applying the boundary conditions to (10),

Figure 1: A finite rod of silicone (white), suspended from a shaker, terminating mass at the bottom surface, one accelerometer attached at each end

using an exponential ansatz.

The length of the rod and the terminating mass were varied.

Beam specimen

The second system was a beam. Since silicone is too limp for a homogenous beam, it was stiffened by two surrounding thin aluminium slats. The cross section is schematically shown in figure 2.

Figure 2: Cross section of the beam specimen: outer layers of aluminium, inner layer of silicone, symmetry in vertical direction

A beam of that cross section was symmetrically mounted on a shaker. Introducing this symmetry, the boundary conditions at the load point were known for the mathematical model. The whole system is schematically shown in figure 3. The beam was excited using maximum-length

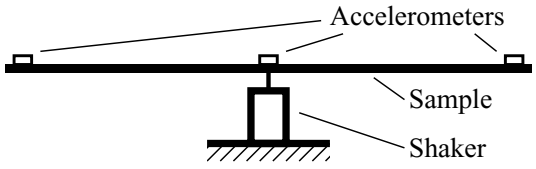

Figure 3: A sandwich beam, symmetrically mounted on a shaker, accelerometers attached

series, which can be transformed to harmonic excitation. The transfer function of acceleration between the load point and the free ends was measured.

No elementary theory exists for such a sandwich beam. So, three Timoshenko beams were kinematically fixed to each other. The vertical displacement w of all layers is identical. The inclinations of the cross sections of the layers are expressed by one of them, e.g. the inclination φ of the inner layer. The equations for the amplitudes $\hat{w}(\Omega, x)$ and $\hat{\varphi}(\Omega, x)$ for harmonic excitation are:

$$\begin{aligned} 0 &= G_o\,(d_o\hat{w}'' - d_i\hat{\varphi}') + \frac{1}{2}d_i\,G_i\,(\hat{w}'' + \hat{\varphi}') \qquad (11)\\ &+ (2\rho_o d_o + \rho_i d_i)\,\Omega^2\hat{w} \\ 0 &= b\,G_o\,(d_o\hat{w}' - d_i\hat{\varphi}) + \frac{1}{2}\,b\,d_i\,G_i\,(\hat{w}' + \hat{\varphi}) \qquad (12)\\ &- \left(C_i I_i - 2C_o I_o\frac{d_i}{d_o}\right)\hat{\varphi}'' - \left(\rho_i I_i - 2\rho_o I_o\frac{d_i}{d_o}\right)\Omega^2\hat{\varphi}, \end{aligned}$$

with the angular frequency Ω, the width of the sample b, the thicknesses of the layers d_o and d_i, the area momenta I_o and I_i, the mass densities ρ_o and ρ_i, the shear moduluses G_o and G_i and the moduluses of plain or uniaxial elongation C_o and C_i. The dependencies of $\hat{w}$ and $\hat{\varphi}$ of Ω and x were not written. Indices o and i denote the outer and inner layers, respectively. This system of ordinary differential equations can be solved using elemental methods.

Results

The identification was started with a small number n of inner variables. After each run of the search algorithm, the number n was increased and the search was restarted. Finally, a set with $n = 8$ was reached.

It is possible to enable the identification of the time constants b_p. This can lead to strange distributions of the b_p, featuring gaps or cumulations on the time interval.

Here, the search for the b_p was disabled and the time constants were defined using $b_p = 10^{p/2}\ s^{-1}$ for all $p = 1, \ldots, 8$ and $b_0 = 0$, as stated above. This distributed them uniformly over the time interval.

The following figures 4 and 5 show the agreement of the measured and calculated transfer functions for one experiment with the rod specimen and for the experiment with the beam specimen, respectively.

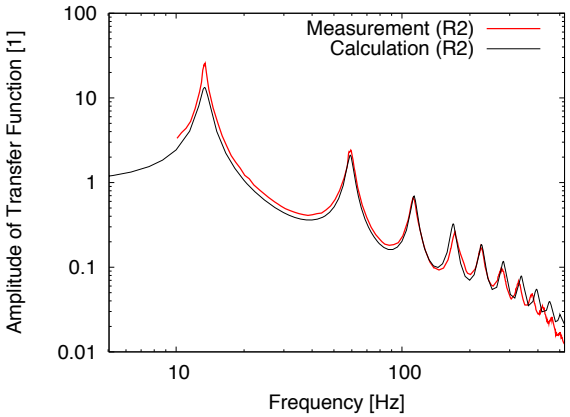

Figure 4: Agreement of measured and calculated transfer functions for the 2nd rod specimen (R2)

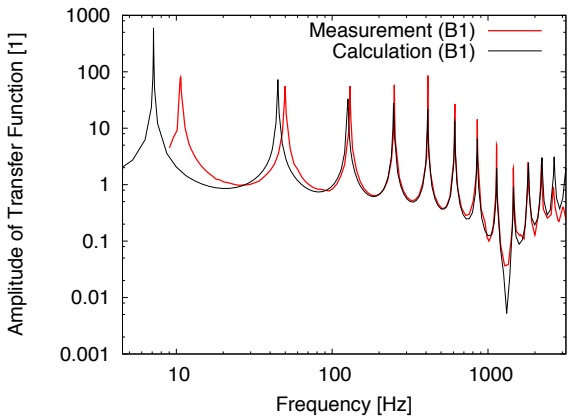

Figure 5: Agreement of measured and calculated transfer functions for the beam specimen (B1)

Overall, the agreement between the measurement and the calculation is good. There are only some small deficiencies concerning the rod specimen at the high frequencies, regarding the matching of the resonance frequencies. At the lowest resonance of about 13 Hz, its amplitude is not adequately met.

Concerning the beam specimen, the three lowest resonance frequencies are not met to a certain degree. The reason for this is seen in the mathematical model used for the sandwich beam which seems too simple for the system. So a future task will be to design a better model, possibly using finite elements for a three-dimensional analysis. Additionally, the amplitudes of the resonances do not always fit. This may result from the fact that the resonances of the beam specimen are very narrow and are therefore not always exactly met by the frequency resolution of the measurement or the calculation.

The figures 6, 7 and 8 show the results of the parameters in the form of the frequency-dependent moduluses, calculated using (7), (8) and (9). In each figure, the real and imaginary parts of the moduluses are given, named storage and loss moduluses, respectively.

The loss moduluses of K, G and E show successive changes throughout the frequency interval given. The amount of variation is a factor of about five for all three cases. The storage moduluses of K and E change only slightly by about 20% over the frequency interval shown. The storage modulus of G changes by a factor of about three.

It is obvious that using a single constant value for the material properties, such as the static moduluses, is hardly a good representation of the dynamic properties measured.

Conclusions

It was shown that using multiple systems for a combined identification of the parameters is possible. This yields one set of parameters which is then valid for the material itself and is not bound to a specific geometry or load.

It was seen that some discrepancies still exist between

the measured and calculated transfer functions for some systems and frequency intervals. It is intended to reduce these discrepancies by the use of more extensive mathematical models. Of course, more time will be required to process them.

Here, the parameters of silicone were identified. Other model scale materials such as acrylic glass and of course real scale materials such as lime-sand brick will be treated using the method presented.

Uncertainties are another important task to work on. They could be given as uncertainties for the parameters K_p, G_p and b_p or for the frequency-dependent moduluses calculated therefrom.

References

[1] C. Kling, "Investigation into Damping in Building Acoustics by Use of Downscaled Models", Diss., RWTH Aachen, 2008

[2] ISO 6721, "Plastics – Determination of dynamic mechanical properties", several parts

[3] DIN 53535, "Testing of rubber – General requirements for dynamic testing", 1982

[4] DIN 53513, "Testing of rubber – Determination of the visco-elastic properties of rubber under forced vibration beyond resonance", 1990

[5] VDI-Richtlinie 3830, "Werkstoff- und Bauteildämpfung", VDI-Verlag, Düsseldorf, 2004–2005

[6] R. Ahrens, "Innere Variablen in linear-viskoelastischen Schwingungssystemen – Modellierung, numerische Behandlung und Parameteridentifikation", Diss., TU Braunschweig, 1993

[7] R. Caracciolo, A. Gasparetto, M. Giovagnoni, "An experimental technique for complete dynamic characterization of a viscoelastic material", Journal of Sound and Vibration, **272** (2004), 1013–1032

[8] M. Schmelzer, "Identifikation der Parameter von Zeitbereichsmodellen linear-viskoelastischer Werkstoffe", Diss., TU Braunschweig, 2004

[9] C. Kling, M. Schmelzer, "Measuring Frequency Dependent Material Properties by Use of N-Parameter Models", Acta Acustica united with Acustica, **94** (2008), 568–579

[10] N.W. Tschoegl, "Time Dependence in Material Properties: An Overview", Mechanics of Time-Dependent Materials, **1** (1997), 3–31

[11] M.E. Gurtin, E. Sternberg, "On the Theory of Viscoelasticity", Arch Rat Mech Anal, **11** (1962), 291–356

[12] S.B. Sane, W.G. Knauss, "On Interconversion of Various Material Functions of PMMA", Mechanics of Time-Dependent Materials, **5** (2001), 325–343

[13] J.A. Nelder, R. Mead, "A Simplex Method for Function Minimization", Comp J, **7** (1965), 308–313

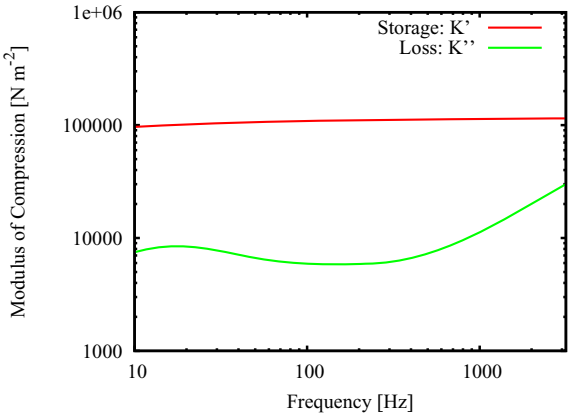

Figure 6: Storage and loss modulus of compression

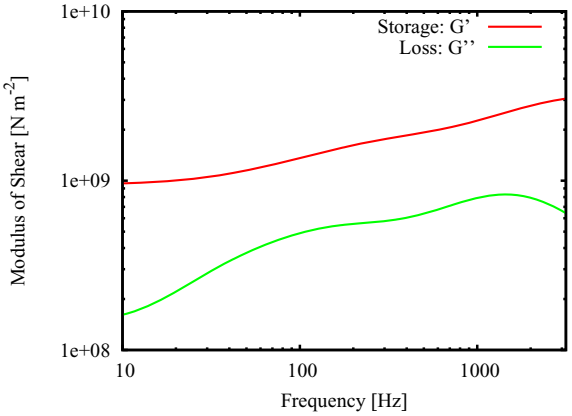

Figure 7: Storage and loss modulus of shear

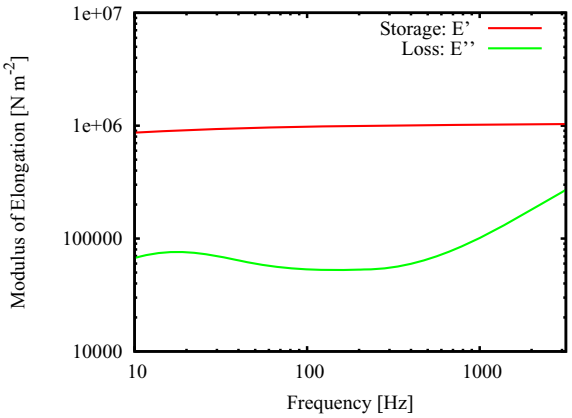

Figure 8: Storage and loss modulus of elongation